Published in IET Generation, Transmission & Distribution
Received on 18th March 2012
Revised on 22nd August 2012
Accepted on 5th September 2012
doi: 10.1049/iet-gtd.2012.0166

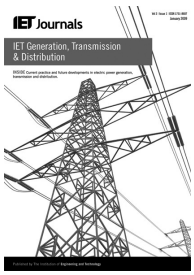

ISSN 1751-8687

Influence of sympathetic inrush on voltage dips caused by transformer energisation

Jinsheng Peng[1], Haiyu Li[1], Zhongdong Wang[1], Foroozan Ghassemi[2], Paul Jarman[2]

[1]School of Electrical and Electronic Engineering, University of Manchester, Manchester M13 9PL, UK
[2]National Grid, Warwick CV34 6DA, UK
E-mail: zhongdong.wang@manchester.ac.uk

Abstract: Energising a transformer with other adjacent transformers in service may induce sympathetic inrush that could lead to long duration voltage dips. This study addresses this issue through analysing voltage dip events observed on a 400/132 kV grid when energisations of several generator step-up transformers were performed. With the help of a number of field measurements of voltage dips involving sympathetic inrush, a detailed network model in alternative transients program/electromagnetic transients program has been developed and validated. Based on the network model, comprehensive simulation studies have been performed. In addition, because of the nature of multiple controlling parameters, sensitivity assessment has been carried out to identify the key influential parameters. It is found that the sympathetic inrush, although does not affect voltage dip magnitude, can prolong voltage dip duration by 143% under the worst energisation condition. The sympathetic inrush occurring in substation transformers gives rise to a network-wide sympathetic interaction, resulting in further prolonged voltage dips on the 132 kV grid. Finally, it is proven that application of static var compensator is able to speed up the voltage dip recovery.

1 Introduction

Power quality is a growing concern for power system operators as well as customers in view of increasing utilisation of sensitive loads, such as variable speed drives and microprocessors [1–3]. One of the main power quality issues is voltage dip (sag) which is defined in the IEC 61000-4-30 as 'temporary reduction of the voltage magnitude at a point in the electrical system below a threshold'. The possible causes of voltage dips can be short-circuit faults, motor starting or transformer energisation. Voltage dips caused by short circuits and motor starting were systematically evaluated [4–6]. During recent years, the voltage dips induced by transformer energisation are gaining more attention [7–14]. In UK, a 3% threshold is normally applied to the voltage dips caused by transformer energisation, and this limit could be further tightened if the interval between consecutive transformer energisations is short, according to Engineering Recommendation P28 (ER-P28) [15].

The characteristics of voltage dips caused by transformer energisation were revealed in [7] that they are non-rectangular (voltage dips recover gradually) and non-symmetrical (each phase has different dip magnitude because of the different degree of saturation). Voltage dips because of energisation of large generator step-up (GSU) transformers for connecting conventional power plants were reported in [8–10]. Specifically, study in [8] investigated voltage dips because of energising a 315 MVA GSU transformer from a 138 kV network and suggested segregated point-on-wave method to minimise voltage dip magnitudes; the dependence of voltage dip magnitudes on network configurations was studied in [9]; the impacts of switching angle, residual flux and system loading condition on voltage dip magnitudes were assessed in [10]. Also, voltage dips caused by energisation of medium-voltage wind turbine transformers were studied in [11–14] to check grid code compliance. With detailed considerations of transformer saturation and upstream network characteristics, all those studies utilised Electro-Magnetic transients program (EMTP) simulation to carry out comprehensive assessments [8–14]. However, most previous studies were devoted to evaluating the magnitude of voltage dips rather than its recovery which could be more important when the transformer inrush is coupled by a phenomenon called sympathetic inrush. A transformer could arouse and engage sympathetic inrush when it is energised into a system where there are adjacent transformers in service. The mechanism of this phenomenon was interpreted in [16] and the key influential factors were evaluated in [17, 18]. With most of the previous studies focusing on its impact on differential protection, recent studies also raised the concerns over its influences on voltage dips [19, 20].

Based on an existing 400 kV transmission grid, this paper investigates the influence of sympathetic inrush on voltage dips that occurred when energisation of large GSU transformers was carried out. Measurements of voltage dip events accompanied by sympathetic interaction between 400 kV GSU transformers are presented. A network model is developed and validated against the field measurement results. It is then used to assess the network-wide impacts of sympathetic interaction on voltage dips and perform

sensitivity studies to identify the key influential parameters. Application of static var compensator (SVC) is also evaluated to show its ability to speed up voltage recovery.

2 System under study and field measurements

A large power plant needs to be connected to a 400 kV transmission grid. As shown in Fig. 1, the grid consists of 11 substations, most of which accommodates a number of autotransformers (400/132/13 kV, 240 MVA, YNa0d11). Substations are linked by 400 kV double circuit transmission lines with lengths ranging from 21 to 97.54 km. There are capacitor banks located at substation *G*, *H* and *B* and SVC devices connected at substation *I*, *E* and *B*. The power plant is located near substation *K*. The coupling circuit breaker CB1 is normally closed. Through power feeder 1, GSU transformers T2 (345 MVA, 400/19 kV, YNd1) and T3 (415 MVA, 400/21 kV, YNd1) are connected to substation busbar via CB2; through power feeder 2, GSU transformer T1 (345 MVA, 400/19 kV, YNd1) is connected via CB3.

To connect the power plant, three steps were conducted: the first step was to energise the GSU transformers to gain power supply from the main grid; the external power supply was then used to start the auxiliary equipments which are necessary for heating up the gas and steam turbines; finally the generators were synchronised. However, the energisation of GSU transformers caused long duration voltage dips which were reported by downstream distribution utilities. Field measurements were therefore conducted for further investigations. Here, two measurement cases involving sympathetic inrush between GSU transformers are illustrated in details.

The first measurement was carried out during the energisation of GSU transformer T1, with T2 and T3 already energised but with secondary side unloaded (it should be noted that in this paper, the current drawn by the energised transformer is named as 'inrush current' and the induced current in adjacent connected transformers is named as 'sympathetic inrush current'). The measured waveforms are shown in Fig. 2 which includes: the three-phase currents observed at power feeder 1 in terms of instantaneous value (Fig. 2*a*) and root mean square (RMS) value (Fig. 2*b*), the voltages measured at substation *K* in term of RMS value (Fig. 2*c*), and three-phase currents measured at the feeder *I–K* which links substation *I* and *K* (as labelled in Fig. 1) in term of instantaneous value (Fig. 2*d*). It should be noted that the calculation of RMS is over one cycle and refreshed every half a cycle, which is in accordance with IEC 61000-4-30. As can be seen in Fig. 2*a*, the no-load magnetising currents become gradually larger after the energisation, which indicate the initiation of sympathetic inrush in GSU transformers T2 and T3. Fig. 2*b* shows that the sympathetic inrush currents took about 2 s to reach their maximum magnitudes (the largest maximum magnitude appeared in phase *C*, which is about 120 A in RMS) and the decay of the sympathetic inrush lasted more than 25 s. In Fig. 2*c*, it can be observed that the system took a long time for a full recovery of voltage for three-phases. The currents measured at feeder *I–K* (shown in Fig. 2*d*) only contain system load currents before transformer energisation; after energisation, they are superimposed by a portion of transformer inrush currents.

The second measurement considered energising GSU transformers T2 and T3 simultaneously, with transformer T1 already energised. The observation point of voltage dips is the same with that in the first measurement. It was also found in the second measurement that the inrush currents decayed very slowly. The recorded maximum dip magnitude at substation *K* was about 32.5 kV on the most affected phase (7.85% of the initial voltage). The voltage dip disturbance lasted about 20 s with the onerous dips lasting about 10 s. It triggered low voltage alarms and led to responses of reactive power compensation devices.

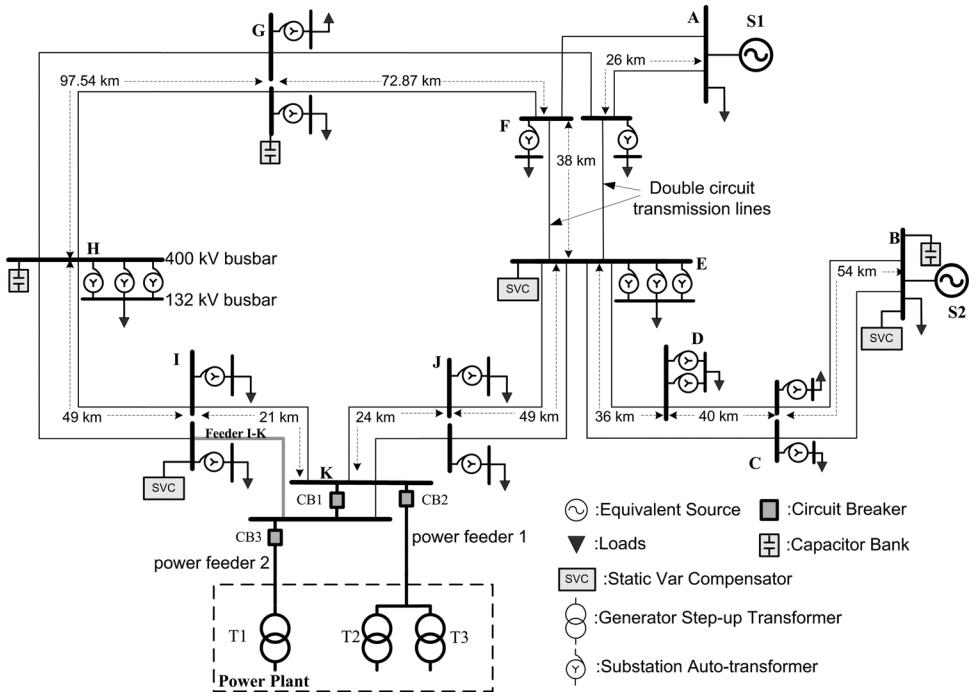

Fig. 1 *Schematic diagram of the system under study*

doi: 10.1049/iet-gtd.2012.0166

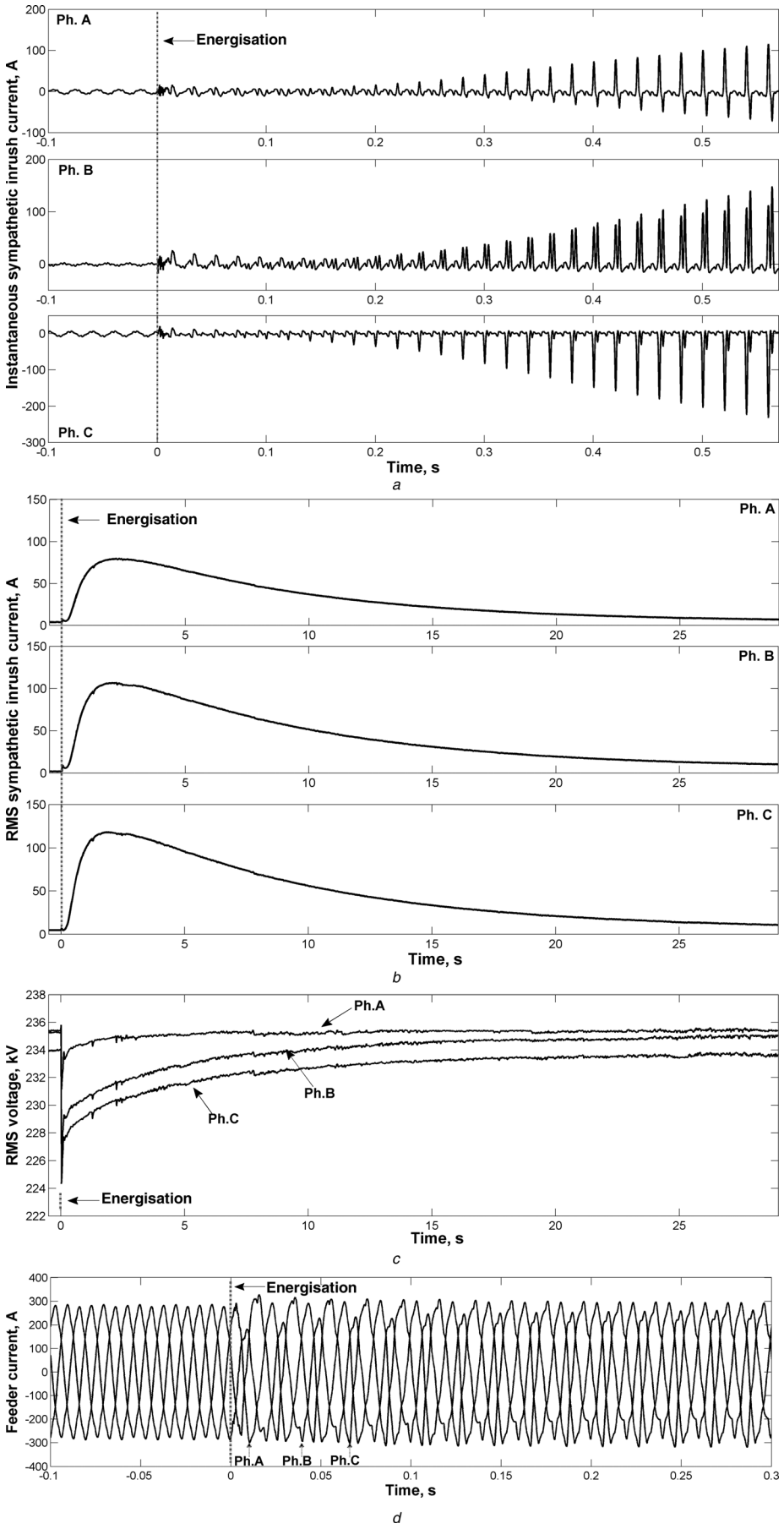

Fig. 2 *Three-phase current and voltage waveforms of the first measurement*

a Instantaneous sympathetic inrush currents
b RMS sympathetic inrush currents
c RMS voltage dips
d Instantaneous currents of feeder *I–K*

3 Sympathetic inrush and voltage dip

The network shown in Fig. 1 can be generically described in Fig. 3*a* by a Thevenin equivalent circuit seen from any of two parallel transformers TE1 and TE2 within the system. The line impedance between TE1 and TE2 is neglected; R_1 and R_2 represent transformer winding resistances; $L_{1\sigma}$ and $L_{2\sigma}$ represent transformer leakage inductances; L_{1m} and L_{2m} are the magnetisation inductances of TE1 and TE2, respectively. $V_s(t)$ is equal to $V_m\sin(\omega t+\theta)$, where V_m is the amplitude of source voltage and θ is the energisation angle; $V_c(t)$ is the voltage of common busbar; $i_s(t)$, $i_1(t)$ and $i_2(t)$ are the currents flowing through supply, TE1 and TE2, respectively.

Applying Kirchhoff's voltage law and Kirchhoff's circuit law, the system can be described by

$$R_s i_s + L_s \frac{di_s}{dt} + R_1 i_1 + \frac{d\lambda_1}{dt} = V_m \sin(\omega t + \theta)$$

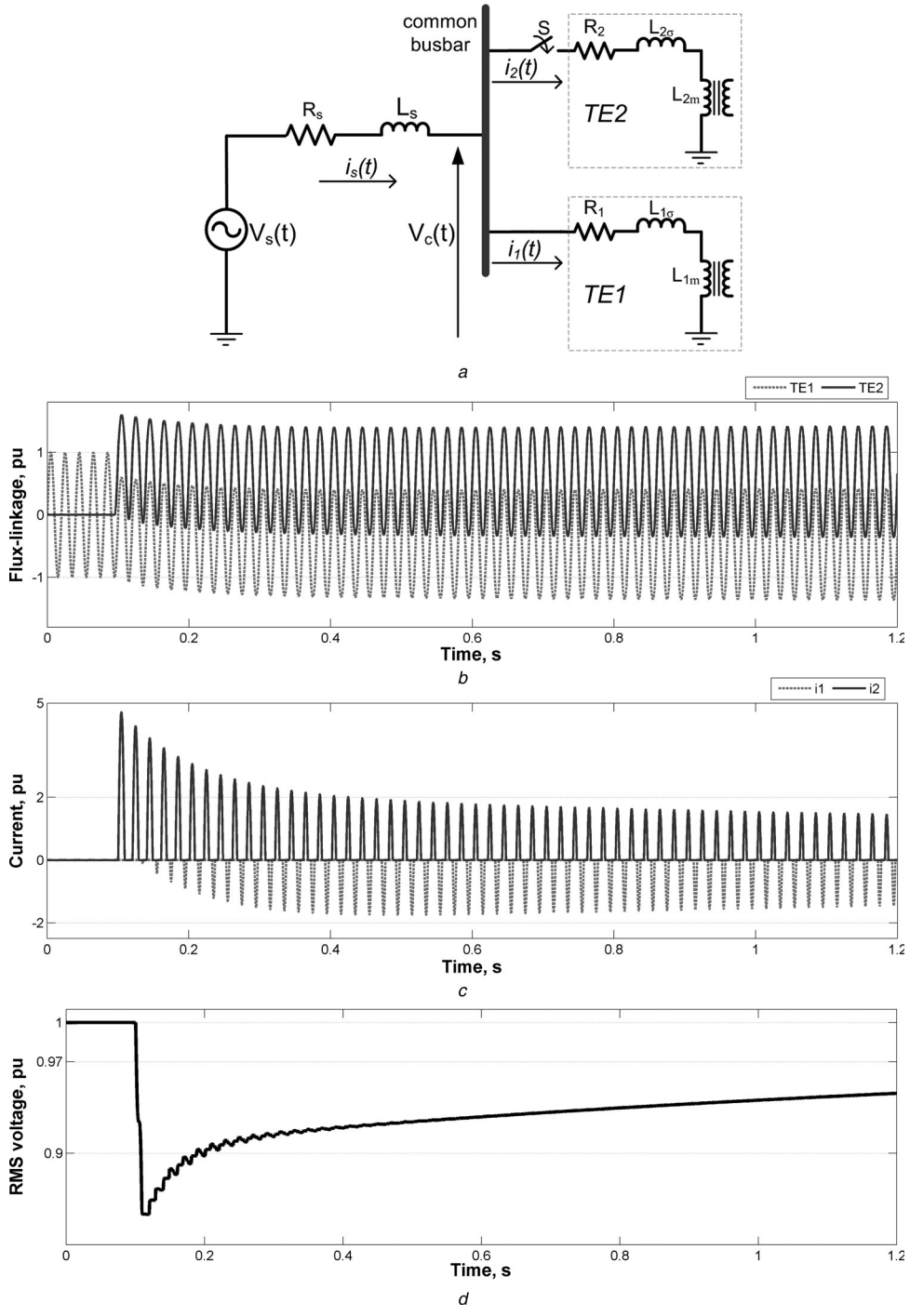

Fig. 3 *Graphical representation*

a Generic power system involving sympathetic interaction between transformers connected in parallel
b Flux-linkages of TE1 and TE2
c Sympathetic inrush currents i_1 and inrush current i_2
d RMS voltage dip at common busbar

doi: 10.1049/iet-gtd.2012.0166

$$R_1 i_1 + \frac{\mathrm{d}\lambda_1}{\mathrm{d}t} = R_2 i_2 + \frac{\mathrm{d}\lambda_2}{\mathrm{d}t}$$
$$i_s = i_1 + i_2 \quad (1)$$

where λ_1, λ_2 are the flux-linkages of TE1 and TE2, respectively, and $\lambda_1 = i_1(L_{1\sigma} + L_{1m})$, $\lambda_2 = i_2(L_{2\sigma} + L_{2m})$.

Owing to the non-linearity of core magnetisation inductances, mathematical solution for (1) cannot be readily obtained. To qualitatively show the sympathetic inrush process, an analysis is made by assuming L_{1m} and L_{2m} to remain constant [21, 22]. Assuming TE1 is identical to TE2, we can obtain $R_1 = R_2 = R$, $L_{1\sigma} + L_{1m} = L_{2\sigma} + L_{2m} = L$. Supposing TE1 has already been energised, energisation of TE2 would induce change of λ_1 and λ_2 as a function of time, which can be expressed by

$$\lambda_1(t) = \frac{L}{Z} V_m \sin(\omega t + \theta - \alpha) - \frac{1}{2}\left[\lambda_1(0) - \lambda_2(0)\right] e^{-((R+2R_s)/(L+2L_s))t} + \frac{1}{2}\left[\lambda_1(0) - \lambda_2(0)\right] e^{-((R/L))t} \quad (2)$$

$$\lambda_2(t) = \frac{L}{Z} V_m \sin(\omega t + \theta - \alpha) - \frac{1}{2}\left[\lambda_1(0) - \lambda_2(0)\right] e^{-((R+2R_s)/(L+2L_s))t} - \frac{1}{2}\left[\lambda_1(0) - \lambda_2(0)\right] e^{-((R/L))t} \quad (3)$$

where $Z = [(R + 2R_s)^2 + (L + 2L_s)^2]^{1/2}$, $\alpha = \arctan[\omega(L + 2L_s)/(R + 2R_s)]$; $\lambda_1(0)$ and $\lambda_2(0)$ are the initial flux of TE1 and the residual flux of TE2, respectively.

From (2) and (3), it can be seen that both $\lambda_1(t)$ and $\lambda_2(t)$ consist of one sinusoidal component and two exponential DC components. The AC component and the first DC component are the same, but the second DC component in λ_1 is opposite to that in λ_2, therefore $i_1(t)$ and $i_2(t)$ are opposite to each other and appear alternately. Also, because the DC components in λ_2 are negative, the maximum peak of $i_2(t)$ would appear right after the energisation of TE2, while the DC components in λ_1 are of opposite polarity and the time constant of the first DC component $\tau_1[= (L + 2L_s)/(R + 2R_s)]$ is smaller than that of the second DC component $\tau_2[= L/R]$, so $i_1(t)$ will gradually reach the maximum peak, and gradually decay afterwards.

The simplified analytical analysis shows in a general way the variation of flux-linkages in TE1 and TE2 which depends on the time constants formed by the inductances and resistances of the circuit branches. In reality, the core inductance is non-linear and therefore the time constants cannot be so readily determined. More accurate estimation of the sympathetic inrush transient can be achieved by using Alternative Transients Program (ATP)/EMTP simulation. Based on the network equivalent parameters and by applying a non-linear saturation curve to magnetisation inductances L_{1m} and L_{2m}, it is possible to simulate the transformer fluxes (λ_1 and λ_2), the currents (i_1 and i_2) and the busbar voltage V_c, as shown in Figs. 3*b*, *c* and *d*, respectively. It can be seen that energisation of TE2 causes asymmetrical distribution of flux-linkages of TE1 and TE2, resulting in inrush current i_2 and sympathetic inrush current i_1; and correspondingly, a significant dip of V_c with slow recovery.

4 Model description and validation

Field measurement results indicate that the system would experience unacceptable long duration voltage dips during energisation of GSU transformers, therefore further studies are required to understand the characteristics of this transient phenomenon. Owing to the difficulty in carrying out more field measurements and the limitations of generic analytical analysis (e.g. the assumption of linear magnetisation inductance), detailed studies can be achieved through computer simulation. This section describes the development of a network model for simulation studies and its validation against the field measurement results.

4.1 Description of network model

The network model was developed using ATP/EMTP based on the 400 kV grid shown in Fig. 1. The sources S1 and S2

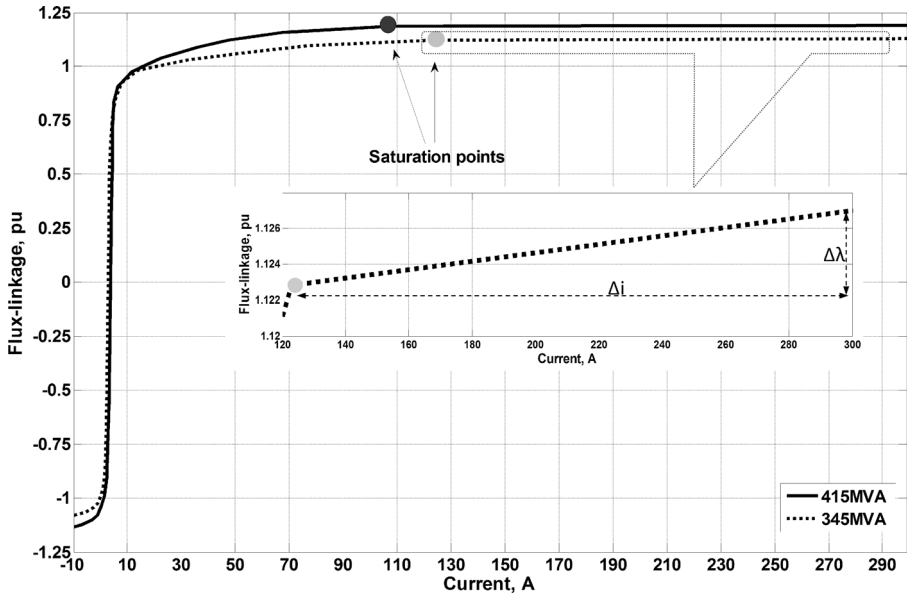

Fig. 4 *Estimated core saturation curves of 415 MVA and 345 MVA GSU transformers*

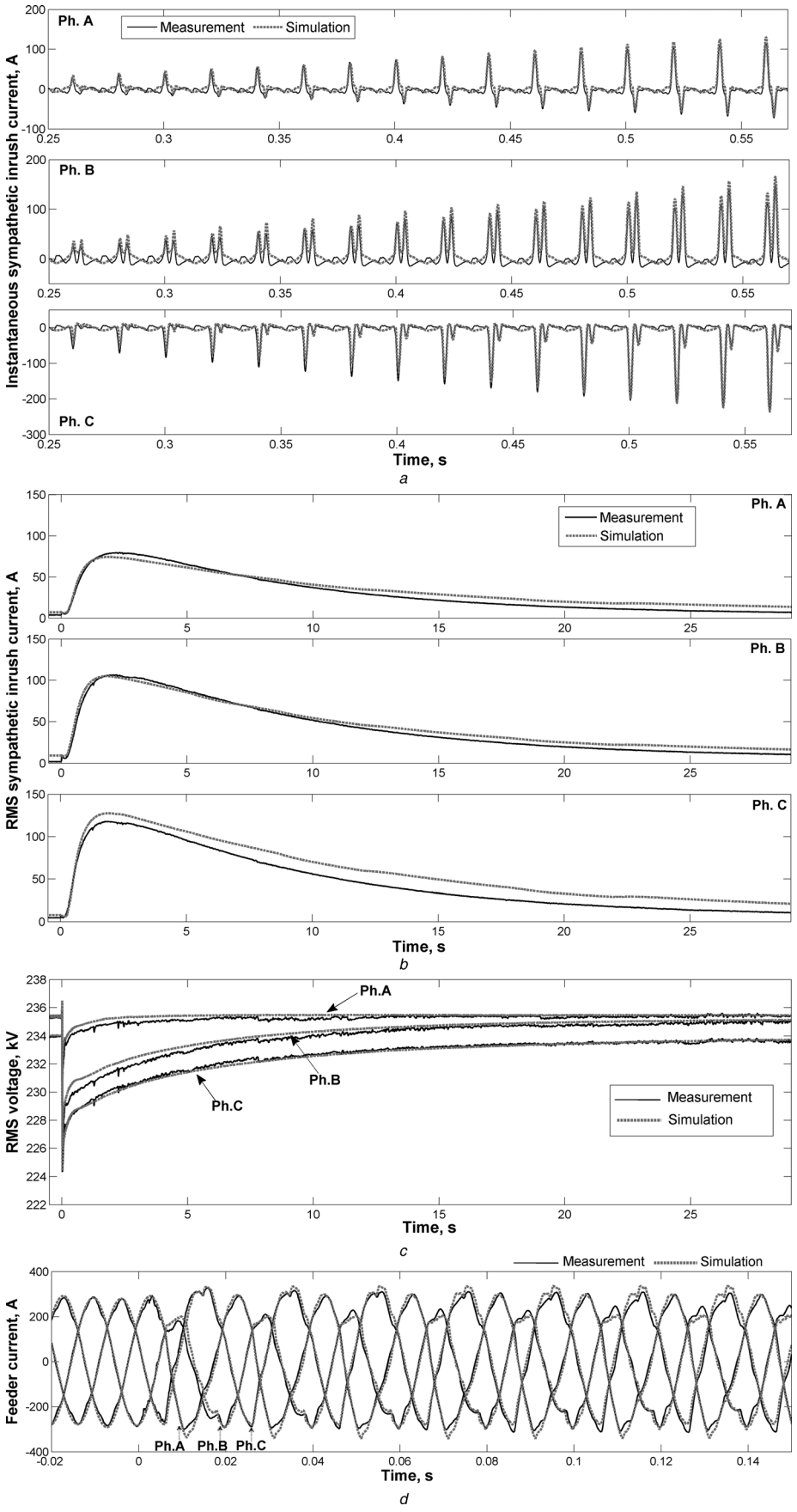

Fig. 5 *Comparison of currents and voltage dips between measured and simulated results*

a Instantaneous sympathetic inrush currents
b RMS sympathetic inrush currents
c RMS voltage dip
d Instantaneous currents of feeder *I–K*

doi: 10.1049/iet-gtd.2012.0166

Table 1 Comparison of three-phase voltage dip magnitudes

Phase	Dip magnitude, kV		Deviation, %
	Field test	Simulation	
A	4.23	4.35	2.8
B	9.28	9.08	2.1
C	9.65	9.6	0.5

are represented by ideal voltage source. Equivalent source impedances to represent source strength are derived from the short-circuit levels at substation *A* and *B* which are 7.1 and 6.4 GVA, respectively. All the double-circuit transmission lines linking the substations are modelled by Bergeron routine, with line dimension, length and transposing scheme taken into account. System loading connected to each substation transformer is modelled by constant lumped impedances connected at 132 kV side, with the power factors of local demands considered. Regarding reactive power compensation devices, all the capacitor banks are modelled by constant capacitor banks rated at 60 MVar; the SVC devices located at substation E and B are modelled by Thyristor controlled reactors rated at 225 MVar in parallel with fixed capacitor banks rated at 150 MVar; the SVC connected at substation *I* is modelled by one tertiary connected Thyristor-switched capacitor with a rating of 60 MVar. The details of the SVC models are not included in this paper, because the model is mainly for validation purpose and for most case studies in following sections, the SVC are not considered, unless otherwise specified.

The modelling of transformer is a main concern. To calculate inrush transients using ATP/EMTP (with ATPDraw as the graphical pre-processor), two types of standard available models are often used, one is BCTRAN and the other is Hybrid Transformer [23, 24]. Owing to the lack of core design data and the need of initialising residual fluxes, BCTRAN was selected to model GSU and substation transformers in this work. Data obtained from test report were used to derive the parameters in transformer model. Based on short-circuit test data, transformer leakage network was represented by $\boldsymbol{RL}^{-1}$ matrix. To approximate core saturation characteristic, open circuit test data were converted by using the algorithm presented in [25, 26] and curve-fitted to form λ–i curves, based on which hysteresis curves were then derived by using a subroutine called HYSDAT [27]. Fig. 4 shows the lower half hysteresis curves for GSU transformers. The saturation points used to define the major hysteretic loop were appointed; beyond the saturation points, the final slopes of saturation curves were quantified by $\Delta\lambda/\Delta i$. Each final slope was determined by the corresponding saturation inductance deduced from transformer air-core inductance, with the effect of winding leakage inductance considered [28]. One assumption adopted here is that air-core inductance is equal to twice the transformer short-circuit inductance [29]. This assumption is reasonable, because, when an unloaded two winding core type transformer is energised from high voltage (HV) winding side (usually the outer winding), the cross-section area of the air-core cylinder enclosed by the HV winding where the flux goes through under deep saturation is normally about twice the cross-section area of the gap between HV and low voltage (LV) winding where the flux goes through during the short-circuit test. These curves were implemented into type-96 non-linear inductors which were then connected in delta and located at the LV terminal to form the core representation [23].

Based on transformer test report data, the approach used to model substation transformers is similar to that applied to modelling GSU transformer T1, T2 and T3, that is, using BCTRAN with externally connected core representation.

4.2 Model validation

Model validation was made according to the first measurement of energisation. The model parameters were obtained as follows: the source voltages were assigned in accordance with the field measurement; source impedances were derived from corresponding system short-circuit level; the amount of system loading at each substation is half of the rated capacity of the substation transformers as stated by the network operator; energisation angles were obtained from the measured voltage waveforms in which three phases were energised simultaneously at 80° (angles are relative to the positive-going zero crossing of phase *A* line-to-ground voltage); transformer air-core inductances are equal to twice of transformer short circuit inductances; because of lack of de-energisation voltage waveform, residual fluxes were assumed zero. Based on these parameter settings, the simulation results were simultaneously generated by the developed network model.

Fig. 5 gives the comparison between simulation and measurement results. In Fig. 5*a*, instantaneous wave shapes of three-phase sympathetic inrush currents were compared, with focus on the initiation of sympathetic inrush. It can be seen that the simulation results can replicate the double-peak patterns, as well as growing trend and peak magnitudes. The build-up and decay of sympathetic inrush were compared in Fig. 5*b* between the simulated RMS sympathetic inrush currents and the field measurement results. Good agreement is achieved in terms of the initiation, the peak instants and magnitudes as well as the decay. Fig. 5*c* illustrates the comparison regarding the long duration RMS voltage dips, with the dip magnitudes particularly compared in Table 1. As can be seen, the simulated voltage dip recovery traces are similar to field measurement results; the biggest deviation of dip magnitude is $<2.9\%$. The comparison in Fig. 5*d* is the currents measured at the feeder *I*–*K*. Good agreement can be seen in

Table 2 Energisation cases and results of phase *C* voltage dips

Case	Sympathetic inrush	GSU transformers being energised	Adjacent GSU transformers in service	RMS voltage dip	
				Magnitude, %	Duration, s
1	no	T1	no	9.6	2.670
2	yes	T1	T2 and T3	9.6	6.479
3	no	T2 and T3	no	18.1	3.376
4	yes	T2 and T3	T1	18.1	7.718

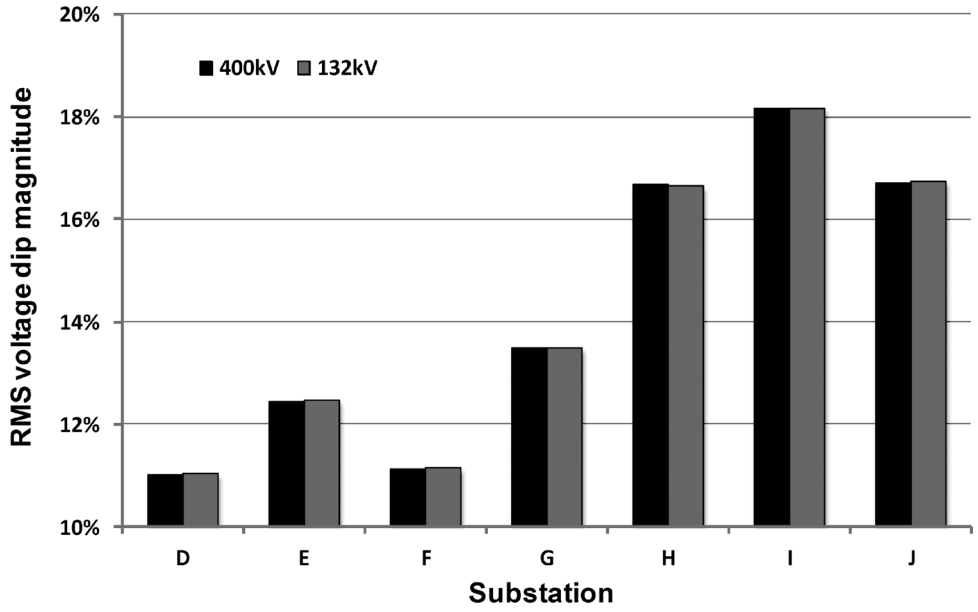

a

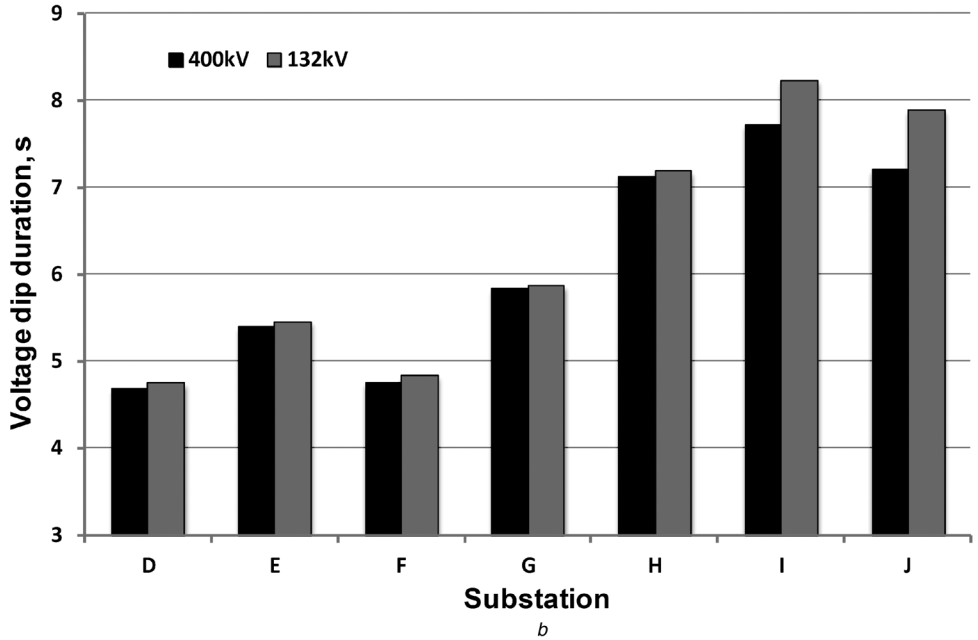

b

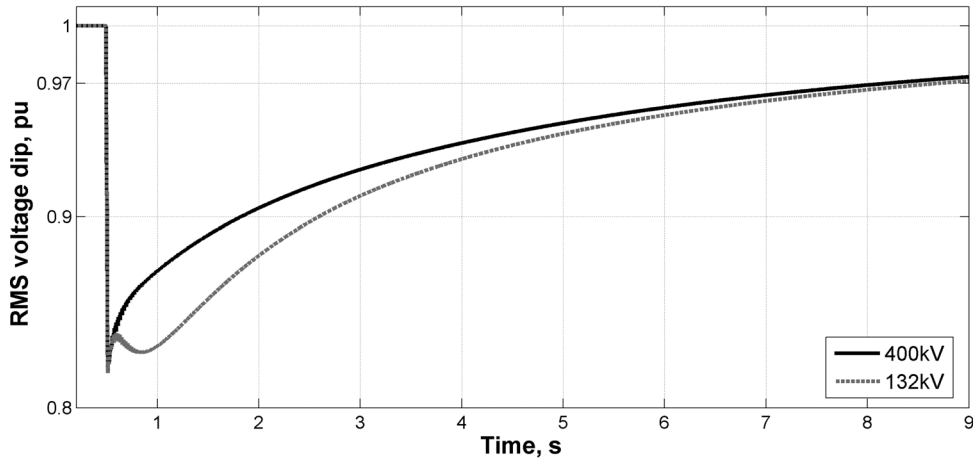

c

Fig. 6 *Voltage dip patterns and recovery traces on 400 kV and 132 kV side*

a Patterns of voltage dip magnitudes across the whole network substations
b Patterns of voltage dip duration
c Voltage dip recovery traces observed at 400 and 132 kV busbars of substation *I*

doi: 10.1049/iet-gtd.2012.0166

the range of steady stage (i.e. prior to energisation), which confirms the correct modelling of system loading. In the range of transient stage (i.e. after energisation), simulation results also show good agreement with field test results. It should be noted that the initial part of voltage recovery was affected by the response of SVC, which has also been correctly replicated in the simulation results. Regarding this SVC effect, more details will be described in Section 7.

In summary, the comparisons show that the network model is capable to replicate measurement results and that the BCTRAN model, although with simple core representation connected externally, is able to simulate the sympathetic inrush transients between transformers. Therefore the network model was employed in following simulation case studies.

5 Effect of sympathetic inrush between GSU transformers

Using the validated model and the same system initial conditions, simulation study was carried out regarding the energisation cases with and without sympathetic inrush between GSU transformers (as shown in Table 2). For all cases, the theoretically worst energisation condition was set as follows: three phases were simultaneously energised at the positive-going zero crossing of phase C line-to-ground voltage; residual flux in phase C is 0.8 pu of peak rated flux (in the direction of flux build-up); residual flux in phase A is -0.8 pu of peak rated flux; and phase B retains zero residual flux [12]. With such energisation conditions, the highest inrush current and biggest voltage dip would appear in phase C. Therefore phase C voltage dips observed at the 400 kV busbar of substation I are shown in Table 2, in terms of dip magnitude and duration. It should also be noted that in the following studies, 3% is taken as the beginning and end threshold for quantifying the duration.

Comparing Cases 1 and 2, it can be seen that the voltage dip magnitudes are the same, however, the dip duration can be prolonged by 143%. Similar observation can be made in the comparison between Cases 3 and 4. By comparing Cases 1 and 3, it can be seen that energising transformers T2 and T3 together would cause voltage dip with longer duration and with magnitude almost twice than that caused by energising T1 alone. However, by comparing Cases 2 and 3, it is shown that the duration of Case 2, which involves energising T1 alone but is influenced by sympathetic inrush, is significantly longer than that of Case 3.

The above case studies show that the sympathetic inrush does not affect the voltage dip magnitude, which is obvious because at the initial stage of the energisation transient, voltage dip is mainly determined by the inrush current in the energised transformers, whereas at this time the sympathetic inrush drawn by the adjacent transformer has yet to build up. With the increase of the sympathetic inrush current, the decay of the inrush current in the energised transformer is slowed down and as a consequence the dip duration is prolonged. The comparisons made between the case studies indicate that this prolonging effect can be very significant.

6 Effect of sympathetic inrush attributed to substation transformers

Based on Case 4, further attempts were made to investigate the sympathetic inrush of substation transformers and the consequent impacts on voltage dip performance. Voltage dip magnitude and duration at 400 and 132 kV substation busbars were observed across the whole network. Fig. 6*a* shows the patterns of voltage dip magnitudes of phase C on both 400 and 132 kV side. It can be seen that the two patterns are almost identical, which indicates that, as far as dip magnitude is concerned, the propagation of voltage dip is not much affected by the substation transformers in the system studied. The dip magnitude observed at each substation is found to be related to the distance between the substation and the supply source and also the distance between the substation and the energised transformers. For those substations (including H, I and J) located in the proximity of the energised transformer and relatively far

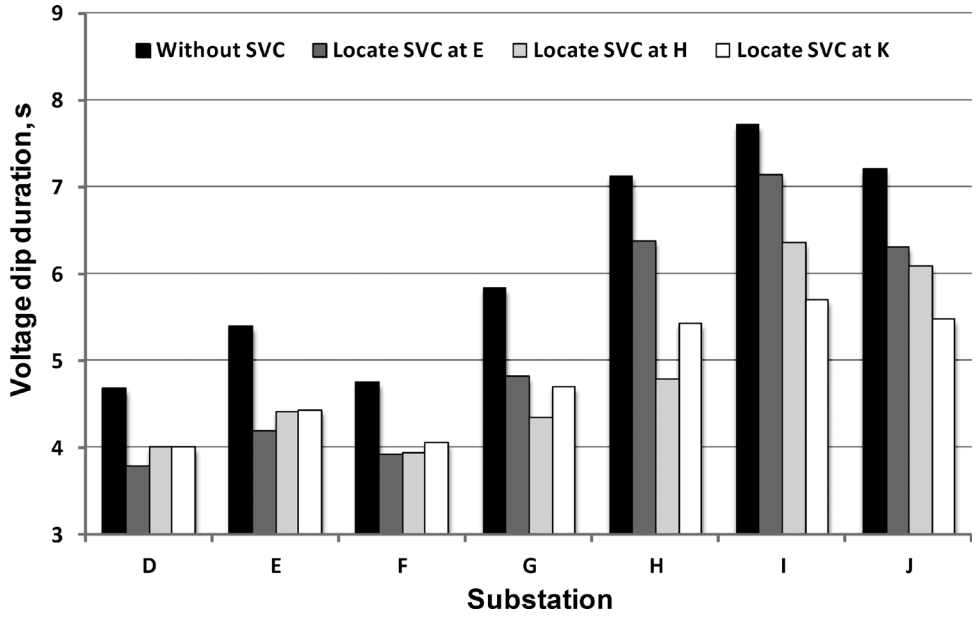

Fig. 7 *Patterns of voltage dip duration at 400 kV side for various SVC locations*

away from supply source, the observed dip magnitudes are relatively large; for those substations (including *D*, *E*, *F* and *G*) located relatively far away from the energised transformer and close to the supply source, the observed dip magnitudes are relatively small.

Fig. 6*b* shows the patterns of voltage dip duration observed on 400 and 132 kV side. It can be seen that the dip durations on 132 kV side are longer. The prolonged voltage dip duration at 132 kV side is attributed to the sympathetic inrush of substation transformers which is further illustrated by voltage dip traces observed at substation *I* shown in Fig. 6*c*. It can be seen that both sides witness the same amount of voltage dip magnitude, however, the recovery at 132 kV side starts to be affected by sympathetic inrush about two cycles after the energisation and continues to be affected for more than 9 s. This effect is found to be related to the distance between substation and the power plant where GSU transformers being energised. For instance, the substation transformers located at substation *I* and *J* have been found the most affected, because of their electrical distances to the GSU transformers are the shortest. The above findings show that, under the worst energisation condition, energisation of large GSU transformers in such systems (characterised by long transmission lines between the supply source and the energised transformers) may trigger a network-wide sympathetic inrush.

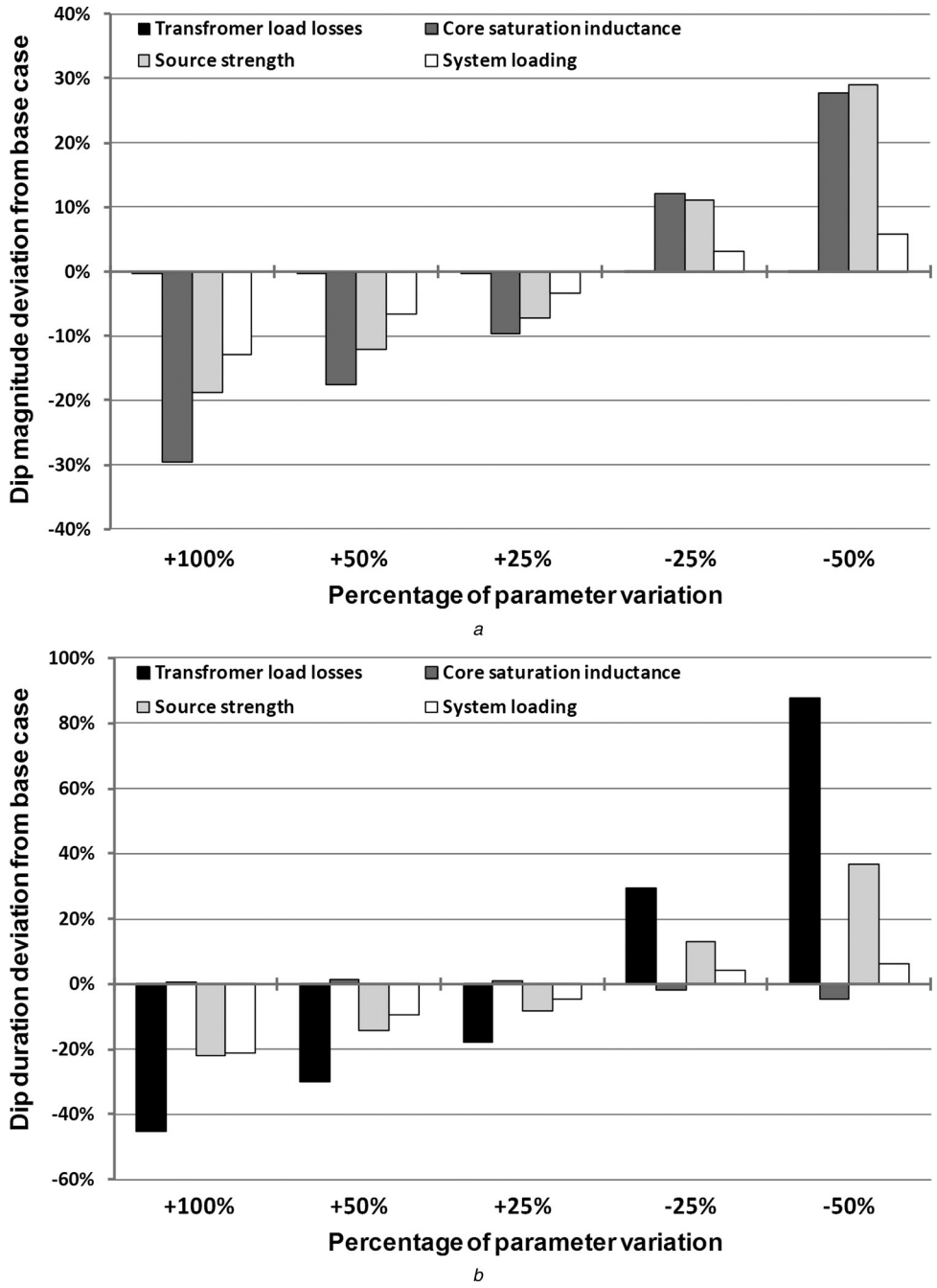

Fig. 8 *Results of sensitivity assessment*

a Impacts of parameter variation on voltage dip magnitude
b Impacts of parameter variation on voltage dip duration

doi: 10.1049/iet-gtd.2012.0166

7 Effect of SVC

The voltage dip recovery performance is further studied when SVC is involved. Here, a set of 300 MVar SVC was applied at different substations and the corresponding voltage dip recovery performance at 400 kV side are shown in Fig. 7. The results suggest that the application of SVC can help speed up the voltage recovery. This effect is influenced by the SVC location. The substations nearest to the SVC location will benefit the most; therefore it is desirable to locate SVC close to the substation where the transformers are energised.

8 Sensitivity assessment

The voltage dips involving sympathetic interaction is influenced by multiple parameters. Sensitivity assessment was carried out to identify the most influential parameters. Here, the concerning parameters include the system source strength, system loading, GSU transformer load losses and GSU transformer core saturation inductance. Switching angle and residual flux were not taken into account in the sensitivity study because they were treated as deterministic parameters forming the worst energisation condition. The sensitivity assessment addresses variations of the concerning parameters between + 100 and − 50%, utilising Case 4 (presented in Table 2) as the base case. Their impacts on 400 kV side voltage dip magnitude and duration are illustrated in Figs. 8*a* and *b*, respectively. In both figures, each column represents the deviation caused by variation of a certain parameter.

Fig. 8*a* illustrates that change of core saturation inductance presents the biggest impact on dip magnitude. The biggest deviation of dip magnitude appears in the case of increasing the core saturation inductance by 100%. Source strength is the second most influential one. In fact, in the reduced cases, the impact of source strength variation on voltage dip magnitude is comparable with that caused by variation of core saturation inductance. The variation of system loading only results in minor impact on dip magnitude. The variation of transformer load losses barely impacts the dip magnitude.

In Fig. 8*b*, it can be observed that change of transformer load losses dominates the impact on voltage dip duration (e. g. 50% reduction of transformer load losses could increase dip duration by 88%); the cases of reduced full-load losses have more impact than those of increased. The second most influential parameter is again the source impedance. 50% reduction of source strength will increase the duration by 36.5%. Variation of system loading only shows minor impact on voltage dip duration, which is similar to its impact on dip magnitude. The variation of core saturation inductance, which exhibits great impact on dip magnitude, however, shows very little impact on voltage dip duration. It should be noted that, although the above analysis focuses on phase *C*, the other two phases also exhibit the same trend.

The minor impact of system loading variation suggests that the system loading condition is of less concern when carrying out transformer energisation in the network studied, which can be attributed to the low ratio of maximum substation loading to the source strength (which is <0.09), that is, the source strength is too strong relative to system loading. However, it is noteworthy that for those systems having a higher ratio of system loading to source strength, the effect of system loading might become more influential. The network studied here is characterised by long transmission lines between supply source and the transformers being energised, and therefore the effect of source strength, to some extent, has been offset by the impedances of long transmission lines; in those systems where the supply source is located closer to the transformers being energised, the impact of source strength variation would be more significant. The variation of core saturation inductance directly influences the magnitude of inrush currents and thus produces great impact on the dip magnitude, but it only slightly affects the decay time constant of inrush transients (because of the relatively small saturation inductance compared with network impedance) and therefore shows little impact on the dip duration. However, most transformers up to date are only tested at factory up to 110%; open circuit test at higher voltages is required for more accurate estimation of core saturation inductance. The significant impact of transformer load losses on dip duration is because the decay of sympathetic inrush is highly determined by the losses of the connection between the GSU transformers and their own losses. Owing to the short electrical distance between the GSU transformers, the amount of load losses of the GSU transformers is the key contributor to the damping of sympathetic inrush and therefore imposes the greatest impact on dip duration.

9 Conclusions

This paper conducts a comprehensive study on the influence of sympathetic inrush on voltage dips caused by transformer energisation based on an existing 400/132 kV network. A number of field measurements of voltage dips involving sympathetic inrush have been carried out, indicating the sympathetic inrush currents can induce long duration voltage dips. A network model was developed in ATP/EMTP and validated against the field measurement results. It is shown that the BCTRAN model, although with simple externally connected core representation, is able to simulate the sympathetic inrush transients between transformers.

Under the worst energisation condition, the validated network model was used to evaluate the degrees of sympathetic interactions between large GSU transformers and between GSU and substation transformers. It is shown that the sympathetic inrush, although does not affect voltage dip magnitude, can prolong voltage dip duration by 143%. The prolonged duration could be more pronounced on 132 kV side, because the sympathetic phenomena extend to substation transformers. It is also shown that application of SVC devices can contribute to speeding up the voltage recovery, and it is more effective by locating SVC closer to the transformers being energised.

Considering sympathetic inrush and voltage dips are controlled by multiple parameters, sensitivity assessment was carried out to identify the most influential parameters on dip magnitude and duration. The amount of transformer load losses has been proven as the key influential parameter to determine the duration of sympathetic inrush and voltage dip. Transformer air-core inductance is found to be most influential on dip magnitude; this parameter, which is normally not available from factory test report, can be estimated using analytical or field calculation or both based on transformer design data; therefore it is suggested that transformer manufacturers provide it in the test report so as to improve the modelling of transformer deep saturation.

10 Acknowledgment

The authors would like to express their sincere gratitude to National Grid for the financial and technical support. The author, Mr. Jinsheng Peng, would like to thank Your Manchester Fund at the University of Manchester for providing Alumni Research Impact Scholarship which partially funds his PhD study.

11 References

1 Sarmiento, H.G., Estrada, E.: 'A voltage sag study in an industry with adjustable speed drives', *IEEE Ind. Appl. Mag*., 1996, **2**, (1), pp. 16–19
2 Kazibwe, W.E., Ringlee, R.J., Woodzell, G.W., Sendaula, H.M.: 'Power quality: a review', *IEEE Comput. Appl. Power*, 1990, **3**, (1), pp. 39–42
3 Lamoree, J., Mueller, D., Vinett, P., Jones, W., Samotyj, M.: 'Voltage sag analysis case studies', *IEEE Trans. Ind. Appl*., 1994, **30**, (4), pp. 1083–1089
4 Heine, P., Lehtonen, M.: 'Voltage sag distributions caused by power system faults', *IEEE Trans. Power Syst*., 2003, **18**, (4), pp. 1367–1373
5 Milanovic, J.V., Aung, M.T., Gupta, C.P.: 'The influence of fault distribution on stochastic prediction of voltage sags', *IEEE Trans. Power Deliv*., 2005, **20**, (1), pp. 278–285
6 Williams, A.J., Griffith, M.S.: 'Evaluating the effects of motor starting on industrial and commercial power systems', *IEEE Trans. Ind. Appl*., 1978, **IA-14**, (4), pp. 292–305
7 Styvaktakis, E., Bollen, M.H.J.: 'Signatures of voltage dips: transformer saturation and multistage dips', *IEEE Trans. Power Deliv*., 2003, **18**, (1), pp. 265–270
8 Nagpal, M., Martinich, T.G., Moshref, A., Morison, K., Kundur, P.: 'Assessing and limiting impact of transformer inrush current on power quality', *IEEE Trans. Power Deliv*., 2006, **21**, (2), pp. 890–896
9 Pors, A., Browne, N.: 'Modelling the energisation of a generator step-up transformer from the high voltage network'. Australasian Universities Power Engineering Conf., Syndey, Australia, December 2008, pp. 1–5
10 Seo, H.C., Kim, C.H.: 'The analysis of power quality effects from the transformer inrush current: a case study of the Jeju power system, Korea'. IEEE PES General Meeting, Pittsburgh, USA, July 2008, pp. 1–6
11 Ma, T., Cadmore, A.: 'System studies of voltage dips resulting from energisation of MV wind turbine transformers'. Int. Conf. and Exhibition on Electricity Distribution, Turin, Italy, 2005, pp. 1–5
12 Smith, K.S.: 'Transformer inrush studies for wind farm grid connections'. Int. Conf. Power Systems Transients, Montreal, Canada, June 2005
13 Arana, I., Holbøll, J., Sørensen, T., Nielsen, A.H., Holmstrøm, O., Sørensen, P.: 'Voltage dip caused by the sequential energization of wind turbine transformers'. Proc. Conf. on European Wind Energy Association, Marseille, France, March 2009
14 Rioual, M., Reveret, J.C.: 'Energization of step-up transformers for wind-farms: modeling and its validation by tests performed on a 10 MW site'. IEEE PES General Meeting, Calgary, Alberta, Canada, 2009, pp. 1–7
15 Engineering Recommendation P28: 'Planning limits for voltage fluctuations caused by industrial, commercial and domestic equipment in the UK' (The Electricity Council, 1989)
16 Bronzeado, H., Yacamini, R.: 'Phenomenon of sympathetic interaction between transformers caused by inrush transients', *IEE Proc., Sci. Meas. Technol*., 1995, **142**, (4), pp. 323–329
17 Kumbhar, G.B., Kulkarni, S.V.: 'Analysis of sympathetic inrush phenomena in transformers using coupled field-circuit approach'. IEEE PES General Meeting, Tampa, Florida, USA, 2007, pp. 1–6
18 Wang, Y.G., Yin, X.G., You, D.H., Xu, T.Q.: 'Analysis on the influencing factors of transformer sympathetic inrush current'. IEEE PES General Meeting, Pittsburgh, USA, July 2008, pp. 1–8
19 Pontt, J., Rodriguez, J., Martin, J.S., Aguilera, R.: 'Mitigation of sympathetic interaction between power transformers fed by long overhead lines caused by inrush transient currents'. IEEE-IAS Annual Meeting, New Orleans, Louisiana, USA, September 2007, pp. 1360–1363
20 Peng, J.S., Ang, S.P., Li, H.Y., Wang, Z.D.: 'Comparisons of normal and sympathetic inrush and their implications toward system voltage depression'. Int. Universities Power Engineering Conf. (UPEC), September 2010, pp. 1–5
21 Bi, D.Q., Wang, X.H., Li, D.J., Yu, G.W., Wang, Z.J., Wang, W.J.: 'Theory analysis of the sympathetic inrush in operating transformers', *Autom. Electr. Power Syst*., 2005, **29**, (6), pp. 1–8
22 Hayward, C.D.: 'Prolonged inrush currents with parallel transformers affect differential relaying', *Trans. Am. Inst. Electr. Eng*., 1941, **60**, (12), pp. 1096–1101
23 Prikler, L., Bánfai, G., Bán, G., Becker, P.: 'Reducing the magnetizing inrush current by means of controlled energization and de-energization of large power transformers', *Electr. Power Syst. Res*., 2006, **76**, (8), pp. 642–649
24 Mork, B.A., Gonzalez, F., Ishchenko, D., Stuehm, D.L., Mitra, J.: 'Hybrid transformer model for transient simulation-part I. development and parameters', *IEEE Trans. Power Deliv*., 2007, **22**, (1), pp. 248–255
25 Neves, W.L.A., Dommel, H.W.: 'Saturation curves of delta-connected transformers from measurements', *IEEE Trans. Power Deliv*., 1995, **10**, (3), pp. 1432–1437
26 Chiesa, N., Hoidalen, H.K.: 'Analytical algorithm for the calculation of magnetization and loss curves of delta-connected transformers', *IEEE Trans. Power Deliv*., 2011, **25**, (3), pp. 1620–1628
27 'ATP rule book' (Leuven EMTP Center, Leuven, Belgium, 1987)
28 Chiesa, N., Mork, B.A., Hoidalen, H.K.: 'Transformer model for inrush current calculations: simulations, measurements and sensitivity analysis', *IEEE Trans. Power Deliv*., 2011, **25**, (4), pp. 2599–2608
29 Povh, D., Schultz, W.: 'Analysis of overvoltages caused by transformer magnetizing inrush current', *IEEE Trans. Power Appar. Syst*., 1978, **PAS-97**, (4), pp. 1355–1365

12 Appendix

The details of GSU transformers rated at 345 and 415 MVA from test reports are given in the following Tables 3 and 4, respectively.

Table 3 GSU transformer test report (T1 and T2, 345 MVA)

Main data	[kV]	[MVA]	[A]	Coupling
HV	400	345	498	YN
LV	19	345	10483	*d*1
open-circuit	E_o, kV,%	[MVA]	I_o, %	P_o, kW
LV	17.1 (90)	345	0.049	126.2
	19 (100)	345	0.103	174.1
	20.9 (110)	345	0.350	239.9
short-circuit	[kV]	[MVA]	Z, %	P_s, kW
HV/LV	400/19	345	17.8	838.4

Table 4 GSU transformer test report (T3, 415 MVA)

Main data	[kV]	[MVA]	[A]	Coupling
HV	400	415	599	YN
LV	21	415	11410	*d*1
open-circuit	E_o, [kV,%]	[MVA]	I_o, [%]	P_o, [kW]
LV	18.9(90)	415	0.05	156.8
	21(100)	415	0.069	211.1
	23.1(110)	415	0.179	290.8
short-circuit	[kV]	[MVA]	Z, %	P_s, kW
HV/LV	400/21	415	17.12	924.7

doi: 10.1049/iet-gtd.2012.0166